EPH/EPHRIN SIGNALING CONTROLS PROGENITOR IDENTITIES IN THE VENTRAL SPINAL CORD

Julien Laussu[1], Christophe Audouard[1], Anthony Kischel[1], Poincyane Assis-Nascimento[2], Nathalie Escalas[1], Daniel J. Liebl[2], Cathy Soula[1] and Alice Davy[1,3]

[1] Centre de Biologie du Développement (CBD), Centre de Biologie Intégrative (CBI), Université de Toulouse, CNRS, UPS, 118 Route de Narbonne, 31062 Toulouse, France

[2]University of Miami Miller School of Medicine. The Miami Project to Cure Paralysis, 1095 NW 14th Terrace, R-48, Miami, FL, USA

[3] corresponding author: alice.davy@univ-tlse3.fr

Running title: Eph signaling in progenitor identity

Keywords: neural progenitors; neural tube; specification; ephrin; boundary

SUMMARY STATEMENT

This article by Laussu et al. describes a role for Eph:ephrin signaling in controlling the identity of neural progenitors in the ventral spinal cord.

ABSTRACT

Early specification of progenitors of the ventral spinal cord involves the morphogen Sonic Hedgehog which induces distinct progenitor identities in a dose-dependent manner. Following these initial patterning events, progenitor identities have to be maintained and propagated faithfully in order to generate appropriate numbers of progeny. Here we provide evidence that local communication via Eph:ephrin signaling is required to maintain progenitor identities at progenitor domain boundaries. We show that ephrinB2 and ephrinB3 are expressed in restricted progenitor domains in the ventral spinal cord while Eph receptors are more broadly expressed. Genetic loss-of-function analyses indicate that expression of ephrinB2 and ephrinB3 is required to control progenitor identities and in vitro experiments reveal that activation of EphA4 in spinal progenitors up-regulates the expression of the identity transcription factor Nkx2.2. Altogether our results indicates that local cell-to-cell communication is necessary to control progenitor identity at domain boundaries.

INTRODUCTION

The vertebrate neural tube is organized along its DV axis in different progenitor domains which first give rise to distinct neuronal subtypes and later on to subtypes of glial cells. Combinatorial information provided by graded Sonic Hedgehog (Shh), Wnt, BMP and FGF signaling induces the regionalized expression of homeodomain and helix-loop-helix transcription factors (TFs) that are specifically expressed in different progenitor domains (Briscoe and Novitch, 2008; Rowitch and Kriegstein, 2010). For instance, progenitors of motor neurons (pMNs) express the identity transcription factor (iTF) Olig2 while adjacent progenitors (p3) which will give rise to v3 interneurons express the iTF Nkx2.2. Ventral patterning of the spinal cord is mainly controlled by the morphogen Sonic Hedgehog (Shh) produced by the notochord and the floor plate (Balaskas et al., 2012 ; Ribes and Briscoe, 2009). It has been shown that in addition to doses, different exposure times to Shh also induces the expression of different sets of TFs in progenitors, thus specifying the distinct progenitor domains (Dessaud et al., 2007). Although the mode of action of Shh at the cellular level is fairly well characterized, one of the unresolved issues in the morphogen field is to completely understand how graded information is translated into the formation of distinct domains with sharp boundaries (Rogers and Schier, 2011). One proposed mechanism is the progressive emergence of a gene regulatory network (GRN) composed of distinct iTFs whose expression is refined by cross-repressive interactions (Balaskas et al., 2012). For instance, a GRN composed of three transcription factors- Pax6, Olig2 and Nkx2.2- is required to interpret graded Shh signaling and to control the position of the boundary between of the p3 and pMN progenitor domains (Dessaud et al., 2008). In addition, expression of these iTFs could be regulated not only by the morphogen signaling pathway but also by other preexisting factors or signaling pathways that may affect interpretation of the morphogen gradient (Rogers and Schier, 2011; Wang et al., 2011). Lastly, additional mechanisms such as cell

sorting could be involved in defining and/or maintaining domain boundaries (Wang et al., 2011; Xiong et al., 2013).

Eph:ephrin signaling is a cell-to-cell communication pathway that has been implicated in numerous developmental processes (Kania and Klein, 2016; Lisabeth et al., 2013). One of its major biological functions is to control cell adhesion and repulsion events in developing and adult tissues thus leading to the establishment and/or maintenance of axon tracts and tissue boundaries (Cayuso et al., 2015; Fagotto et al., 2014). In addition, Eph:ephrin signaling has also been shown to control various aspects of neural progenitors development and homeostasis in the cortex including self-renewal, proliferation, quiescence and differentiation (Laussu et al., 2014). In the developing spinal cord, Eph:ephrin signaling has been prominently studied in post-mitotic neurons, specifically in axon guidance and fasciculation of motor neurons (Kao et al., 2011; Luxey et al., 2013; Luxey et al., 2015), as a consequence, virtually nothing is known on the function of this pathway in spinal progenitors. Here, we questioned the role of Eph:ephrin signaling in specifying progenitor domains in the ventral spinal cord.

RESULTS

EphrinB2 and ephrinB3 are expressed in complementary domains in progenitors of the ventral spinal cord

A survey of B-type ephrins expression in the mouse ventral spinal cord (Figure 1A) indicated that *Efnb2* and *Efnb3* are expressed in ventral spinal progenitors from E9.5 to E11.5 (Figure 1B). *Efnb1* presents a diffuse expression decreasing over time in the ventral spinal cord and has not been considered further in this study (Figure 1B). In addition to a strong expression in motor neurons (MN), a low *Efnb2* expression was detected in spinal progenitors (Figure 1B). Because the expression of *Efnb2* in progenitors of the ventral neural tube was barely

detectable by in situ hybridization we took advantage of a reporter mouse line that expresses H2BGFP under the control of the *Efnb2* endogenous promoter (Davy and Soriano, 2007; Luxey et al., 2015) to confirm this expression pattern. The benefit of this reporter strategy is that H2BGFP accumulates in the nucleus thus highlighting low domains of expression and facilitating co-expression analyses. In accordance with in situ hybridization data, H2BGFP expression was detected in a restricted population of neural progenitors from E9.5 to E11.5 (Sup Figure 1). In situ hybridization revealed high *Efnb3* expression in a ventral-most domain of the spinal cord and a lower expression more dorsally from E9.5 to E11.5 (Figure 1B). In addition to its restricted expression in progenitors, *Efnb3* is also expressed in MN at E11.5 (Figure 1B). To examine whether restricted expression of *Efnb2* and *Efnb3* corresponds to populations of progenitors with a defined identity, we performed co-staining with the iTFs Olig2 and Nkx2.2 to detect pMN and p3 progenitors, respectively. This revealed that the ventral boundary of *Efnb2:H2BGFP* expression strictly matched the p3/pMN boundary (Figure 1C). On the other hand, the dorsal boundary of H2BGFP expression does not correspond to the dorsal boundary of Olig2 expression (Sup Figure 1). Conversely, in situ hybridization analyses coupled with immunostaining for Olig2 revealed that the highest level of *Efnb3* expression corresponds to the floor plate and p3 progenitors and that *Efnb3* is expressed at a low level in pMN progenitors (Figure 1D). Together, these expression analyses revealed that ephrinB2 and ephrinB3 have complementary expression patterns in pMN and p3 progenitors, respectively.

Eph forward signaling is active in spinal progenitors.

EphrinB2 and ephrinB3 are able to bind EphB1, EphB2, EphB3 and EphA4 with differing affinities (Blits-Huizinga et al., 2004). In situ hybridization and immunostaing showed that all

four Eph receptors are expressed in progenitors of the ventral neural tube as well as in MN at E10.5, with slightly differing expression patterns and expression levels (Figure 2A, B). Eph receptor tyrosine kinases are signaling molecules and one hallmark of their activation is phosphorylation on key tyrosine residues. To assess how the differential expression patterns of Eph and ephrins translated into signaling pathway activation within the developing neural tube, we assessed EphBs and EphA4 phosphorylation using antibodies specific to these key phosphorylated tyrosine residues. Unexpectedly, while EphBs and EphA4 exhibit a broad distribution in ventral progenitors and differentiating MN (Figure 2A, B), phosphorylated forms of EphBs and EphA4 exhibited a much more restricted distribution (Figure 2C). The phospho-EphB signal was detected as clusters concentrated close to the apical surface of progenitors and was also detected in MN soma, highlighted by the higher expression of *Efnb2:H2BGFP* (Luxey et al., 2015). The phospho-EphA4 signal was detected at the apical surface of progenitors with a strong dorsal enrichment (Figure 2C). Surprisingly, no P-EphA4 signal was detected in MN soma, despite the high expression of EphA4 in these cells (Figure 2A, B). Immunostaining with Nkx2.2 to highlight the pMN/p3 boundary shows that neither P-EphBs nor P-EphA4 is preferentially enriched at this boundary (Figure 2C). Because the restricted localization of phosphorylated Eph receptors was unexpected, we sought to validate the in vivo specificity of these phospho-specific antibodies using gain of function experiments in the chick neural tube. To do this, we electroporated a truncated version of ephrinB3 lacking its cytoplasmic domain (which retains its ability to activate forward signaling) and assessed phosphorylation of EphBs and EphA4 after 24 h. EphrinB3$^{\Delta Cter}$ electroporation led to an increased signal detected by both phospho-specific antibodies on the electroporated side of the neural tube, which is consistent with the expected steady-state activation of these receptors (Sup Figure 2). Altogether these results show that phosphorylated Eph receptors are

present in progenitors of the ventral neural tube indicating that Eph forward signaling is active in these cells.

EphrinB3 but not ephrinB2 is required to segregate p3 and pMN progenitors.

One of the well characterized function of Eph:ephrin signaling is to maintain developmental boundaries, thus regulating tissue patterning. Given the restricted expression of ephrinB2 and ephrinB3 in pMN and p3 progenitors, we asked whether Eph:ephrin signaling was required for the maintenance of the p3/pMN boundary. To do this we generated *Efnb2* and *Efnb3* mutant embryos. *Efnb2*$^{-/-}$ embryos exhibit precocious lethality (E10.5) due to cardiovascular defects (Adams et al., 1998; Wang et al., 1998) prompting us to generate *Efnb2* conditional mutant embryos to analyze later stages of development. We used the *Olig2-Cre* mouse line to excise *Efnb2* in the motor neuron lineage, starting in pMN progenitors from E9.5 (*Efnb2*$^{lox/lox}$*; Olig2-Cre* thereafter called cKO). On the other hand, *Efnb3* knock-out embryos (*Efnb3*$^{-/-}$ thereafter called KO) are viable and were used for all our analyses. We thus examined the distribution of Olig2+ and Nkx2.2+ cells in E11.5 *Efnb3* KO and *Efnb2* cKO. To do this in a quantitative manner, we measured surfaces encompassing all Olig2+ or Nkx2.2+ nuclei on transverse sections and deduced their region of overlap (Figure 3). We then quantified the proportion of sections presenting an overlap and we measured the surface of overlap. In *Efnb2* cKO, no overlap between Olig2+ and Nkx2.2+ domains was detected in *Efnb2* cKO (Figure 3). In contrast, in *Efnb3* KO both the proportion of sections presenting an overlap and the surface of overlap between Olig2+ and Nkx2.2+ domains were increased (Figure 3) highlighting the presence of Olig2+/Nkx2.2- progenitors in the p3 domain. These results indicate that ephrinB3, but not ephrinB2, is required to segregate p3 and pMN progenitors.

EphrinB2 and ephrinB3 play opposite roles in defining the number of pMN and p3 progenitors.

There are two (non exclusive) possible causes for the phenotype described above: 1) p3 and pMN progenitors are specified normally in *Efnb3* KO but the lack of ephrinB3 expression ventrally causes progenitors intermingling ; and 2) specification of p3 and pMN progenitors is altered in absence of ephrinB3 with ventral progenitors failing to acquire and/or maintain Nkx2.2 expression. To discriminate between these two possibilities, we reasoned that a specification defect may create an imbalance in p3 and pMN numbers. We thus quantified the number of Olig2+ and Nkx2.2+ spinal progenitors at two developmental stages in ephrin mutants. First we analyzed *Efnb2*$^{-/-}$ and *Efnb3*$^{-/-}$ complete knock out embryos at E9.5, a stage at which p3 and pMN patterning is dependent on Shh. No differences were observed in the distribution or number of Olig2+ or Nkx2.2+ progenitors in either mutant at E9.5 (Figure 4A). A small fraction of nuclei expressed both Olig2+ and Nkx2.2+ (progenitors of mixed identity) and this was also unchanged in absence of ephrinB2 or ephrinB3. These results show that early specification of ventral neural progenitors does not require ephrinB2 and ephrinB3 expression. Next, we quantified the number of Olig2+ and Nkx2.2+ progenitors at E11.5 in *Efnb2* cKO, *Efnb3* KO and in control embryos. First we compared E9.5 and E11.5 control embryos. As expected from previous studies, we observed a decrease of the number of Olig2+ progenitors and an increase in Nkx2.2+ progenitors while the total number of p3+pMN progenitors slightly increased from E9.5 to E11.5 in control embryos (Figure 4A, B). Next we compared control and mutant embryos at E11.5. Remarkably, *Efnb3* KO exhibit an increase in the number of Olig2+ progenitors balanced by a significant decrease in the number of Nkx2.2+ progenitors compared to control embryos (Figure 4B). Importantly, no change in the number of progenitors with a mixed identity or in the total number of p3+pMN progenitors was observed in *Efnb3* KO (Figure 4B), suggesting that loss of ephrinB3 modifies the ratio

between Olig2+ and Nkx2.2+ progenitors without affecting their proliferation and/or differentiation. Strikingly, an opposite phenotype to that of *Efnb3* KO was observed in *Efnb2* cKO, with a reduction in the number of Olig2+ progenitors which was balanced by an increase in the number of Nkx2.2+ progenitors (Figure 4B). Again, in *Efnb2* cKO, the number of progenitors with mixed identity and the total number of p3+pMN progenitors was unchanged (Figure 4B), suggesting a change in identity from Olig2+ to Nkx2.2+ in absence of ephrinB2, rather than a change in proliferation or differentiation. To support this interpretation, we performed BrdU incorporation and immunostaining for the neuronal marker Islet1/2 which showed that proliferation and differentiation rates of Olig2+ progenitors were unchanged in *Efnb2* cKO compared to control embryos (Sup Figure 3). Importantly, using in situ hybridization, we observed no difference in *Shh* expression in *Efnb2* or *Efnb3* mutants compared to wild type embryos (Sup Figure 4). Despite the fact that the change in progenitor identity in *Efnb2* cKO affected a relatively small fraction of Olig2+ progenitors, this led to a reduction in motor neurons numbers at later developmental stages (Figure 5). Similarly, in *Efnb3* KO the increase in the number of pMN correlated with an increased number of motor neurons (Figure 5). This data supports the interpretation that the observed changes in progenitor numbers are not due to altered differentiation, since MN and pMN numbers remain proportional in mutant embryos.

Lastly, to confirm the role of Eph:ephrin signaling in specification events, we tested for a potential genetic interaction between *Efnb2* and *Shh*, since previous reports have shown that similar to ephrinB2, Shh signaling is required to maintain pMN identity after initial patterning (Allen et al., 2011; Allen et al., 2007; Dessaud et al., 2010). We generated compound heterozygous embryos and quantified p3 and pMN progenitors at E11.5. While the number of Olig2+ and Nkx2.2+ progenitors in $Efnb2^{+/-}$ and $Shh^{+/-}$ heterozygous embryos was equivalent to wild type embryos (Figure 6), $Efnb2^{+/-}$; $Shh^{+/-}$ trans-heterozygous embryos exhibited a

phenotype similar to *Efnb2* cKO embryos, with a switch from Olig2+ to Nkx2.2+ identity (Figure 6). These results demonstrate that *Efnb2* and *Shh* interact genetically to maintain pMN identity in the ventral neural tube.

Collectively, these results indicate that ephrinB2 and ephrinB3, which are differentially expressed in pMN and p3 progenitors, are required to maintain and/or propagate these respective progenitor identities after initial specification events. In addition, ephrinB3 plays a role in segregating p3 and pMN progenitors.

Eph forward signaling controls iTF expression.

One of the main outcomes of Shh signaling in progenitors of the ventral neural tube is to control the expression of iTFs in a dose dependent manner, respectively Nkx2.2 and Olig2 in p3 and pMN progenitors. We reasoned that one possible mechanism of action of Eph:ephrin signaling may be in the regulation of the expression of these iTFs. To test this we turned to primary spinal progenitors cultured in vitro which allow us to test changes in gene expression following acute Eph signaling activation. In growing conditions these cells express the iTFs Olig2 and Nkx2.2 while the MN markers Islet 1/2 and Foxp1 are expressed at low level (Figure 7A, B). In addition, qRT-PCR analyses revealed that EphA4 (but not EphB1-3) is prominently expressed in these cells while expression of ephrinB2 and ephrinB3 is undetectable (Figure 7B). To test whether activation of EphA4 may regulate iTF expression, we incubated dissociated spinal progenitors in pre-clustered recombinant EfnB2-Fc or EfnB3-Fc for 2 hours to activate forward signaling. We then performed qRT-PCR analyses to monitor the expression of various genes relevant to Shh signaling and p3 and pMN specification. Incubation with recombinant pre-clustered EphB2-Fc was used as a control treatment. Stimulation of EphA4 with either EfnB2-Fc or EfnB3-Fc led to the upregulation of

Nkx2.2, while the expression of *Olig2* was not changed (Figure 7C). As expected, no change in gene expression was detected in cells exposed to EphB2-Fc (Figure 7C). Altogether, these results show that acute activation of EphA4 leads to upregulation of the iTF *Nkx2.2* in spinal progenitors which is consistent with a role for Eph:ephrin signaling in controlling progenitor identity.

DISCUSSION

While early steps of ventral neural tube patterning have been extensively studied, highlighting the critical role of Shh, mechanisms that ensure fidelity in the maintenance and/or propagation of these ventral progenitor identities over time are less well characterized. Recent genetic studies indicate that continuous Shh signaling is required to maintain p3 and pMN identities since mouse mutants in which Shh signaling is altered exhibit a progressive loss of Olig2, and to a lesser extent Nkx2.2, expression (Allen et al., 2011; Dessaud et al., 2010). Here we identified Eph:ephrin signaling as a novel mechanism required to maintain and/or propagate the identity of these progenitors after initial patterning steps. We propose that expression of ephrinB2 and ephrinB3, respectively in pMN and p3 progenitors, is necessary to maintain the expression of Olig2 and Nkx2.2 in these cells. Because of the existing repressive regulatory loop between Olig2 and Nkx2.2 (Balaskas et al., 2012), modulation of Nkx2.2 expression impacts on the expression of Olig2 expression (and vice versa) thus controlling the ratio between p3 and pMN identities. Other signaling pathways have been shown to act in cooperation or in opposition to Shh to control p3 and pMN specification, including Wnt and Notch signaling (Alvarez-Medina et al., 2008; Kong et al., 2015; Robertson et al., 2004; Wang et al., 2011 ; Yu et al., 2008).

We observed that cells changing identity in absence of Eph:ephrin signaling represent a small fraction of p3 and pMN progenitors, the majority of which maintain a correct identity in ephrin mutants. Further, these cells are located close to the p3/pMN boundary, as evidenced by a shift in dorso-ventral positioning of this boundary in ephrin mutants (data not shown). A similar small dorsal shift of this boundary has been reported in *Olig2*$^{-/-}$ embryos (Balaskas et al., 2012), suggesting that only progenitors located close to the p3/pMN boundary change fate even in complete absence of Olig2. These observations suggest that Eph:ephrin signaling is required to precisely control the identity of progenitors which are located in regions of non discriminant morphogen concentrations. Indeed, progenitors located on either side of the p3/pMN boundary are exposed to similar doses of morphogen yet they faithfully maintain and/or propagate their distinct identities in control embryos. Our results indicate that upon loss of ephrinB2 or ephrinB3 a fraction of these progenitors are mis-specified, acquiring the identity of cells across the boundary. On the other hand, progenitors located away from the boundary are unaffected by the loss of Eph:ephrin signaling, possibly because they are continuously exposed to distinctive doses of morphogen.

Traditionally, the role of Eph:ephrin signaling in specification processes has been linked to its function in boundary maintenance. For instance, a recent study has shown that loss of ephrinB2 in the developing cochlea leads to a switch in cell identity from supporting cell to hair cell fate and this was attributed to the mis-positioning of supporting cells into the hair cell layer (Defourny et al., 2015). Our results are not consistent with this interpretation since changes in the ratio between p3 and pMN progenitors observed in *Efnb2* and *Efnb3* mutants is opposite what would be expected from mis-positioning of progenitors. Instead, our data suggest that Eph signaling regulates specification by directly controlling the expression of iTFs. This conclusion is consistent with a growing number of published studies reporting a role for Eph:ephrin signaling in lineage commitment or cell fate maintenance via the

modulation of intracellular signal transduction pathways and gene expression, independently of cell sorting at boundaries (Ashton et al., 2012; Chen et al., 2016; Haupaix et al., 2013; Ottone et al., 2014; Picco et al., 2007; Stolfi et al., 2011). Nevertheless, our data shows that in *Efnb3* mutants, progenitors are mis-specified and mis-positioned, indicating that ephrinB3 plays a dual role in specification and sorting of spinal progenitors.

Our genetic data shows that expression of ephrinB2 is required to maintain the pMN fate in two different genetic contexts (*Shh*$^{+/-}$ and *Olig2-Cre*$^{+/-}$), yet the expression of *Olig2* was not modified in response to short-term EphA4 activation, even when we used EfnB2-Fc to stimulate EphA4. It may thus be possible that ephrinB2 acts in *cis* instead of *trans* -interaction with EphA4, as was previously reported in spinal motor axon guidance (Kao and Kania, 2011).

Phosphorylation of Eph receptors on specific tyrosine residues is generally considered a hallmark of activation. Immunostaining with phospho-specific antibodies revealed receptor phosphorylation in pMN and p3 progenitors, consistent with receptor activation and one of the puzzling results of our study is the finding that phosphorylated EphA4 and EphB2 are enriched at the apical membrane of neural progenitors. The mechanisms underlying the subcellular localization of phosphorylated Eph receptors or its significance for downstream signaling are currently unknown. Of note, we show here that expression and phosphorylation patterns of Eph receptors are quite distinct in the ventral neural tube, indicating that extrapolation from expression to pathway activation must be done with caution when studying in vivo contexts.

In conclusion, our study indicates that Eph forward signaling exerts its specification function in the ventral spinal cord through a “community effect” (consolidating same identity in neighbors within domains) rather than through a “lateral inhibition effect” (inducing a different identity in neighbors across boundary), which is counter-intuitive to its well-known

repulsive effect (separating neighbors of different identities). More generally, our study opens the way to further discoveries on the role of Eph:ephrin signaling in refining morphogen-dependent tissue patterning.

MATERIALS AND METHODS

Mice

Ephrin mutant mice were maintained in a mixed background and genotyped by PCR. The mouse lines *Shh*^{ko}, *Efnb3*^{ko}, *Efnb2*^{lox} and *Efnb2*^{GFP} have been described previously (Davy and Soriano, 2007; Grunwald et al., 2004; Yokoyama et al., 2001). The *Olig2-Cre* mouse line (Dessaud et al., 2007) was maintained in a pure C57Bl6/J genetic background. For *Efnb2* cKO, control genotypes used in the study include *Efnb2*$^{lox/lox}$, *Efnb2*$^{lox/GFP}$, *Efnb2*$^{+/GFP}$ and *Efnb2*$^{+/GFP}$*; Olig2-Cre*. For *Efnb3* KO, control genotypes are always *Efnb3*$^{+/-}$. E0.5 is defined as the day on which a vaginal plug was detected. All animal procedures were pre-approved by the institution ethical committee (protocol number: MP/07/21/04/11).

In Situ Hybridization

In situ hybridization was performed using standard protocols on 70µm vibratome sections at brachial level. Antisense RNA probes labeled with digoxigenin were used to detect in vivo gene expression with a 72 h incubation time.

Immunostaining

All analyses for *Efnb2* cKO were performed on control and mutant littermates collected from at least two different litters. On the other hand, control and *Efnb3* mutant embryos were collected from independent litters. The number of embryo analyzed for each immunostaining and each developmental stage is indicated in the figure legends. To avoid bias in rostro-caudal

axis, data was collected on thick vibratome sections covering the entire brachial region (600 μm). Antibody staining was performed following standard protocol on 70μm vibratome sections of mouse and chick embryos at brachial level. For BrdU incorporation, pregnant dams were injected with BrdU (10mg/ml; 100mg/kg) with intraperitoneal injection. After 1 h, embryos were dissected in cold PBS and processed for subsequent immunostaining.

Antibodies used were: goat anti-Nkx2.2 (1/100, Santa Cruz Biotechnology); rabbit anti-Olig2 (1/1000, Sigma); mouse anti-Islet1/2, 39-4D5 (1/50, DSHB); rabbit anti-Foxp1 (1/200, Abcam), rabbit anti-P-H3 (1/1000, Millipore), rabbit anti-EphA4 (1/100, Santa Cruz Biotechnology), goat anti-EphB2 (1/50, R&D Systems), rabbit anti-phosphoEphA4 (1/100, a gift from Dr Greenberg), rabbit anti-phosphoEphBs (1/100, Abcam), Tuj1 (1/1000, Covance). All secondary antibodies were from Jackson ImmunoResearch (1/1000).

Image processing and quantification

Images were collected on a Leica SP5 confocal microscope or Nikon eclipse 80i microscope for *in situ* hybridization data. Cell numbers were collected blindly on 5 vibratome sections (n=25 confocal Z-sections) per embryo and at least 2000 nuclei were recorded per embryo. The number of embryo analyzed for each immunostaining and each developmental stage is indicated in the figure legends. Acquisitions of nuclei 2D positions and semi quantitative analyses of fluorescence intensity were performed using Fiji (Schindelin et al., 2012). Spatial distribution of progenitor subtypes was quantified using the R Project (http://www.r-project.org/), see Supplementary Information (Sup Code) for details on the code.

Spinal progenitor primary cultures

Spinal progenitor stem cells were obtained from spinal cord of E12.5 mouse embryos. Briefly, spinal cords were dissociated in ice cold HBSS solution and transferred to pre-warmed

DMEM/F12. Single cell suspension was obtained by mechanical dissociation of pooled tissues. Cells were centrifuged at 1500 rpm and resuspended in pre-warmed cell culture medium freshly prepared (DMEM/F12 supplemented with 1.5 mM Putrescine, 5 mM Hepes, 3 mM NaHcO3, penicillin-streptomicin, 1x B27 supplement, 1x N2 supplement, 1x ITSS, 5 ng/ml FGF, 20 ng/ml EGF, 30% glucose). Cell culture medium was refreshed every 2-3 days by adding 10 % fresh medium. Spinal progenitor stem cells grown in suspension form "neurospheres" which were dissociated every 2 weeks using 0.25% Trypsin solution, diluted 1/3 and transferred to fresh cell culture medium.

For stimulations, neurospheres were dissociated with mild trypsine treatment and cells were incubated for 2 h at 37°C with 1 µg/ml pre-clustered IgG-Fc, EfnB3-Fc (or EfnB2-Fc) or EphB2-Fc in full medium. RNA was extracted from cell pellets using TRI-reagent according to the manufacturer's instructions. 1 µg RNA was used for reverse transcription. Genomic DNA was degraded with 1 µl DNAse (RQ1, ROCHE) for 20 min at 37°C in 20 µl RNAse, DNAse-free water (W4502-Sigma) and the reaction stopped by adding 1 µl STOP solution under heat inactivation at 65°C for 10 min. Two µl dNTPS (10mM, Promega) and 2 µl oligdTs (100mM, idtDNA) were added for 5 min at 65°C then 8 µl 5X buffer, 2 µl Rnasin (N2511-ROCHE) and 4 µl 100mM DTT (Promega) were added for 2 min at 42°C. The mix was then divided in equal volumes in a RT negative control tube with addition of 1 µl water and in a RT positive tube with 1 µl superscript enzyme (Invitrogen) and placed at 42°C for 1 h. Reaction was stopped at 70°C for 15 min. cDNAs were diluted (10-fold, 100-fold and 1000-fold) and processed for quantitative PCR in triplicate for each dilution. 10 µl diluted cDNAs was mixed with 10 µl premix Evagreen (BTIU31019, VWR) containing 1 µmM of each primers and PCR program run for 35 cycles on a MyiQ BioRad thermocycler. mRNA relative expression levels were calculated using the 2-ddCts method. For stimulation analyses, relative level of expression were normalized to *S16* and to the IgG-Fc condition.

Expression constructs and in ovo electroporation

Mouse cDNA coding for the truncated version of ephrinB3 lacking its cytoplasmic domain (deletion of 85 amino acids) was cloned into the bicistronic pCIG (IRES-EGFP) expression vector (Megason and McMahon, 2002). Fertilized chicken eggs (local supplier, France) were incubated at 38°C in a humidified incubator for appropriate periods to yield E3 embryos. DNA constructs (1µg/µl) were electroporated using a homemade electroporator (based on Philips PM5705 pulse generator) into the neural tube of E3 chick embryos. Electroporated embryos were dissected, fixed and processed for immunostaining 24 h later.

Statistical Analysis

For all analyses sample size was estimated empirically. Sample sizes are indicated in figure legends and further details are provided in Sup Table 1. Statistical analyses were performed with GraphPad, using unpaired two-way Student *t*-test, Mann-Whitney test or ANOVA, depending on the data set. $P<0.05$ was considered statistically significant. *P* values provided in the Figures are for Student t-test, with the following notation: *$P<0.05$; **$P<0.01$; ***$P<0.001$, ns= non significant. Details on statistical analyses and *P* values are provided in Sup Table 2.

ACKNOWLEDGEMENTS

The Islet 1/2 antibody was obtained from the Developmental Studies Hybridoma Bank developed under the auspices of the NICHD and maintained by the University of Iowa, Iowa City, IA 52242. We thank Dr Novitch and Dr Jessell for sharing the *Olig2-Cre* mice and Dr Grunwald for the *Efnb2*^{loxlox} mice. We are greatful to Dr Greenberg for sharing the phospho-EphA4 antibody. Dr Kania and Dr Henkemeyer provided some molecular reagents used in

this study. We are grateful to Brice Ronsin for his help with confocal microscopy (TRI Imaging Core Facility) and to Marion Aguirrebengoa for her help with statistical analyses. We thank the ABC facility and ANEXPLO for housing mice. We are grateful for Sylvain Touret's help for writing the R code. We thank Eric Agius for critical reading of the manuscript.

COMPETING INTERESTS

The authors declare no conflict of interest.

AUTHOR CONTRIBUTIONS

JL planned, performed and analyzed experiments, and he participated in writing the manuscript; CA, AK and NE performed and analyzed experiments; PA and DL collected and provided *Efnb3* mutant embryos and revised the manuscript; CS provided scientific input on the project and revised the manuscript; AD supervised the project, planned the experiments, analyzed the data and wrote the manuscript.

FUNDING

Research in the Davy team is financed by the CNRS, by the Fondation ARC and by ANR (ANR-15-CE13-0010-01). JL received support from the French Ministère de l'Enseignement Supérieur et de la Recherche and from the Fondation pour la Recherche Médicale (FDT20140931010). DJL is funded by the Miami Project to Cure Paralysis and PAN by NIH/NINDS (NS089325).

REFERENCES

Adams, R. H., Wilkinson, G. A., Weiss, C., Diella, F., Gale, N. W., Deutsch, U., Risau, W. and Klein, R. (1998). Roles of ephrinB ligands and EphB receptors in cardiovascular development: demarcation of

arterial/venous domains, vascular morphogenesis, and sprouting angiogenesis. *Genes Dev.* **13**, 295-306.

Allen, B. L., Song, J. Y., Izzi, L., Althaus, I. W., Kang, J. S., Charron, F., Krauss, R. S. and McMahon, A. P. (2011). Overlapping roles and collective requirement for the coreceptors GAS1, CDO, and BOC in SHH pathway function. *Dev Cell* **20**, 775-87.

Allen, B. L., Tenzen, T. and McMahon, A. P. (2007). The Hedgehog-binding proteins Gas1 and Cdo cooperate to positively regulate Shh signaling during mouse development. *Genes Dev* **21**, 1244-57.

Alvarez-Medina, R., Cayuso, J., Okubo, T., Takada, S. and Marti, E. (2008). Wnt canonical pathway restricts graded Shh/Gli patterning activity through the regulation of Gli3 expression. *Development* **135**, 237-47.

Ashton, R. S., Conway, A., Chinmay, P., Bergen, J., Kwang-Il, L., Shah, P., Bissell, M. and Schaffer, D. V. (2012). Astrocytes regulate adult hippocampal neurogenesis through ephrin-B signaling. *Nat. Neurosci.* **15**, 1399-1407.

Balaskas, N., Ribeiro, A., Panovska, J., Dessaud, E., Sasai, N., Page, K. M., Briscoe, J. and Ribes, V. (2012). Gene regulatory logic for reading the Sonic Hedgehog signaling gradient in the vertebrate neural tube. *Cell* **148**, 273-284.

Blits-Huizinga, C. T., Nelersa, C. M., Malhotra, A. and Liebl, D. J. (2004). Ephrins and their receptors: binding versus biology. *IUBMB Life* **56**, 257-65.

Cayuso, J., Xu, Q. and Wilkinson, D. G. (2015). Mechanisms of boundary formation by Eph receptor and ephrin signaling. *Dev Biol*.

Chen, S., Bremer, A. W., Scheideler, O. J., Na, Y. S., Todhunter, M. E., Hsiao, S., Bomdica, P. R., Maharbiz, M. M., Gartner, Z. J. and Schaffer, D. V. (2016). Interrogating cellular fate decisions with high-throughput arrays of multiplexed cellular communities. *Nat Commun* **7**, 10309.

Davy, A. and Soriano, P. (2007). Ephrin-B2 forward signaling regulates somite patterning and neural crest cell development. *Dev. Biol.* **304**, 182-193.

Defourny, J., Mateo Sanchez, S., Schoonaert, L., Robberecht, W., Davy, A., Nguyen, L. and Malgrange, B. (2015). Cochlear supporting cell transdifferentiation and integration into hair cell layers by inhibition of ephrin-B2 signalling. *Nat Commun* **6**, 7017.

Dessaud, E., Ribes, V., Balaskas, N., Yang, L. L., Pierani, A., Kicheva, A., Novitch, B. G., Briscoe, J. and Sasai, N. (2010). Dynamic assignment and maintenance of positional identity in the ventral neural tube by the morphogen sonic hedgehog. *PLoS Biol* **8**, e1000382.

Dessaud, E., Yang, L. L., Hill, K., Cox, B., Ulloa, F., Ribeiro, A., Mynett, A., Novitch, B. G. and Briscoe, J. (2007). Interpretation of the sonic hedgehog morphogen gradient by a temporal adaptation mechanism. *Nature* **450**, 717-20.

Fagotto, F., Winklbauer, R. and Rohani, N. (2014). Ephrin-Eph signaling in embryonic tissue separation. *Cell Adh Migr* **8**, 308-26.

Grunwald, I. C., Korte, M., Adelmann, G., Plueck, A., Kullander, K., Adams, R. H., Frotscher, M., Bonhoeffer, T. and Klein, R. (2004). Hippocampal plasticity requires postsynaptic ephrinBs. *Nat. Neurosci.* **7**, 33-40.

Haupaix, N., Stolfi, A., Sirour, C., Picco, V., Levine, M., Christiaen, L. and Yasuo, H. (2013). p120RasGAP mediates ephrin/Eph-dependent attenuation of FGF/ERK signals during cell fate specification in ascidian embryos. *Development* **140**, 4347-4352.

Kania, A. and Klein, R. (2016). Mechanisms of ephrin-Eph signalling in development, physiology and disease. *Nat Rev Mol Cell Biol*.

Kao, T. J. and Kania, A. (2011). Ephrin-mediated cis-attenuation of Eph receptor signaling is essential for spinal motor axon guidance. *Neuron* **71**, 76-91.

Kao, T. J., Law, C. and Kania, A. (2011). Eph and ephrin signaling: Lessons learned from spinal motor neurons. *Semin. Cell Dev. Biol.* **23**, 83-91.

Kong, J. H., Yang, L., Dessaud, E., Chuang, K., Moore, D. M., Rohatgi, R., Briscoe, J. and Novitch, B. G. (2015). Notch activity modulates the responsiveness of neural progenitors to sonic hedgehog signaling. *Dev Cell* **33**, 373-87.

Laussu, J., Khuong, A., Gautrais, J. and Davy, A. (2014). Beyond boundaries: Eph/ephrin signaling in neurogenesis. *Cell Adh Migr.* **8**, 349-359.
Lisabeth, E. M., Falivelli, G. and Pasquale, E. B. (2013). Eph Receptor Signaling and Ephrins. *Cold Spring Harb Perspect Biol.* **5**, a009159.
Luxey, M., Jungas, T., Laussu, J., Audouard, C., Garces, A. and Davy, A. (2013). Eph/ephrin-B1 forward signaling controls fasciculation of motor and sensory axons. *Dev. Biol.* **383**, 264-274.
Luxey, M., Laussu, J. and Davy, A. (2015). EphrinB2 sharpens lateral motor column division in the developing spinal cord. *Neural Dev* **10**, 25.
Megason, S. G. and McMahon, A. P. (2002). A mitogen gradient of dorsal midline Wnts organizes growth in the CNS. *Development* **129**, 2087-98.
Ottone, C., Krusche, B., Whitby, A., Clements, M., Quadrato, G., Pitulescu, M. E., Adams, R. H. and Parrinello, S. (2014). Direct cell-cell contact with the vascular niche maintains quiescent neural stem cells. *Nature cell biology* **16**, 1045-56.
Picco, V., Hudson, C. and Yasuo, H. (2007). Ephrin-Eph signaliing drives the asymmetric division of notochord/neural precursors in *Ciona* embryos. *Development* **134**, 1491-1497.
Robertson, C. P., Braun, M. M. and Roelink, H. (2004). Sonic hedgehog patterning in chick neural plate is antagonized by a Wnt3-like signal. *Dev Dyn* **229**, 510-9.
Schindelin, J., Arganda-Carreras, I., Frise, E., Kaynig, V., Longair, M., Pietzsch, T., Preibisch, S., Rueden, C., Saalfeld, S., Schmid, B. et al. (2012). Fiji: an open-source platform for biological-image analysis. *Nat Methods* **9**, 676-82.
Stolfi, A., Wagner, E., Taliaferro, J. M., Chou, S. and Levine, M. (2011). Neural tube patterning by Ephrin, FGF and Notch signaling relays. *Development* **138**, 5429-5439.
Wang, H., Lei, Q., Oosterveen, T., Ericson, J. and Matise, M. P. (2011). Tcf/Lef repressors differentially regulate Shh-Gli target gene activation thresholds to generate progenitor patterning in the developing CNS. *Development* **138**, 3711-3721.
Wang, H., Lei, Q., Oosterveen, T., Ericson, J. and Matise, M. P. (2011). Tcf/Lef repressors differentially regulate Shh-Gli target gene activation thresholds to generate progenitor patterning in the developing CNS. *Development* **138**, 3711-3721.
Wang, H. U., Chen, Z.-F. and Anderson, D. J. (1998). Molecular distinction and angiogenic interaction between embryonic arteries and veins revealed by ephrin-B2 and its receptor eph-B4. *Cell* **93**, 741-753.
Xiong, F., Tentner, A. R., Huang, P., Gelas, A., Mosaliganti, K. R., Souhait, L., Rannou, N., Swinburne, I. A., Obholzer, N. D., Cowgill, P. D. et al. (2013). Specified neural progenitors sort to form sharp domains after noisy Shh signaling. *Cell* **153**, 550-561.
Yokoyama, N., Romero, M. I., Cowan, C. A., Galvan, P., Helmbacher, F., Charnay, P., Parada, L. F. and Henkemeyer, M. (2001). Forward signaling mediated by ephrin-B3 prevents contralateral corticospinal axons from recrossing the spinal cord midline. *Neuron* **29**, 85-97.
Yu, W., McDonnell, K., Taketo, M. M. and Bai, C. B. (2008). Wnt signaling determines ventral spinal cord cell fates in a time-dependent manner. *Development* **135**, 3687-96.

FIGURE LEGENDS

Figure 1. EphrinB2 and ephrinB3 are expressed in complementary domains in progenitors of the ventral spinal cord.

A. Schematic representation of progenitor domains in the ventral spinal cord. B. Expression of *Efnb1* (a-c), *Efnb2* (d-f) and *Efnb3* (g-i) was monitored by in situ hybridization on transverse sections of E9.5, E10.5 and E11.5 embryos, as indicated. Brackets indicate domains of low expression of *Efnb2*. Scale bars: 50 μm. C. Transverse sections of *Efnb2*$^{+/GFP}$ E11.5 embryos were immunostained to detect Olig2 (a) and Nkx2.2 (b). Epifluorescence is shown on (c) and a merged image is shown on (d). The dashed line marks the p3/pMN boundary. Scale bars: 50 μm. D. Transverse sections of wild type E10.5 embryos were processed first for *Efnb3* in situ hybridization (b) and second for Olig2 immunostaining (a). A merged image is shown on (c). The dashed line marks the p3/pMN boundary. Scale bars: 25 μm. E. Schematic representation of *Efnb2* and *Efnb3* expression in relation to pMN and p3 progenitors domains.

Figure 2. Eph forward signaling is active in progenitors of the ventral spinal cord.

A. Expression of *EphB1* (a), *EphB2* (b), *EphB3* (c) and *EphA4* (g-i) was monitored by in situ hybridization on transverse sections of E10.5 (a-c) or E11.5 (d) embryos. Scale bars: 50 μm. B. Transverse sections of E10.5 embryos were immunostained to detect EphA4 (a, red), EphB2 (b, blue) and differentiated neurons (Tuj1, green in c). Scale bars: 40 μm. C. Transverse sections of E10.5 *Efnb2*$^{+/H2BGFP}$ embryos were immunostained to detect phospho-EphBs (a, c, e, red) or phospho-EphA4 (b, d, f, red) and co-immunostained with Nkx2.2 (c-f, blue). Expression of H2BGFP is shown by epifluorescence (c-f, green). Single channel images showing immunostaining with phospho-specific antibodies are shown in a, b. Scale bars: 40 μm (a-d); 20 μm (e, f).

Figure 3. Olig2+ progenitors are mis-positioned in the p3 domain in *Efnb3*$^{-/-}$ embryos.

Transverse sections of a control (a), *Efnb2* cKO (b) and *Efnb3*$^{-/-}$ (c) E11.5 embryos were immunostained to detect Olig2 (red) and Nkx2.2 (blue). Example of spatial positioning of Olig2+ and Nkx2.2+ progenitors in a non-overlap control situation (d) and in an overlap situation (e). Quantification of the proportion of sections showing an overlap in control and *Efnb2* cKO embryos (f). Quantification of the surface of overlap between Olig2+ and Nkx2.2+ domains in control and *Efnb2* cKO embryos (g). Quantification of the proportion of sections showing an overlap in *Efnb3*$^{+/-}$ and *Efnb3*$^{-/-}$ embryos (h). Quantification of the surface of overlap between Olig2+ and Nkx2.2+ domains in *Efnb3*$^{+/-}$ and *Efnb3*$^{-/-}$ embryos (i). Error bars indicate s.e.m.; n=5 embryos per genotype; *$P<0.05$ (unpaired two-sample *t*-tests). ns: non significant. Scale bars: 50 μm.

Figure 4. EphrinB2 and ephrinB3 play opposite roles in regulating the number of p3 and pMN progenitors.

A. Transverse sections of wild type (a), *Efnb2*$^{-/-}$ (b) and *Efnb3*$^{-/-}$ (c) E9.5 embryos were immunostained to detect Olig2 (red) and Nkx2.2 (blue). The number of Olig2+, Nkx2.2+ and Olig2+/Nkx2.2+ (double) progenitors was quantified for the 3 genotypes (n=3 embryos per genotype). B. Transverse sections of *Efnb3*$^{+/-}$ (a), *Efnb3*$^{-/-}$ (b), *Efnb2*$^{lox/GFP}$ (c) and *Efnb2*$^{lox/GFP}$*;Olig2-Cre* (d) E11.5 embryos were immunostained to detect Olig2 (red) and Nkx2.2 (blue). The number of Olig2+, Nkx2.2+ and Olig2+/Nkx2.2+ (double) progenitors was quantified in *Efnb3*$^{+/-}$ and *Efnb3*$^{-/-}$ embryos (e) and in *Efnb2*$^{lox/GFP}$ and *Efnb2*$^{lox/GFP}$*; Olig2-Cre* embryos (f) (n=5 embryos per genotype) (f). For both graphs, total refers to the sum of Olig2+ and Nkx2.2+ progenitors. Error bars indicate s.e.m.; **$P<0.01$; ***$P<0.001$ ns= non significant (unpaired two-sample *t*-tests).

Figure 5. EphrinB2 and ephrinB3 inversely control motor neuron numbers.

A. Transverse sections of E12.5 *Efnb2*$^{lox/GFP}$ (a) and *Efnb2*$^{lox/GFP}$*; Olig2-Cre* (b) embryos were immunostained to detect Foxp1 (red) and Islet 1/2 (blue). Quantification of the total number of motor neurons (Foxp1+ and Islet 1/2+) in both genotypes (c). The repartition of motor neurons in motor columns is not affected by loss of ephrinB2 (d). B. Transverse sections of E12.5 *Efnb3*$^{+/-}$ (a) and *Efnb3*$^{-/-}$ (b) embryos were immunostained to detect Foxp1 (red) and Islet 1/2 (blue). Quantification of the total number of motor neurons (Foxp1+ and Islet 1/2+) cells in both genotypes (c). The repartition of motor neurons in motor columns is not affected by loss of ephrinB3 (d). Error bars indicate s.e.m.; n=6 embryos per group; **P*<0.05; ***P*<0.01; ****P*<0.001; ns= non significant (unpaired two-sample *t*-tests). Scale bar: 50 mm.

Figure 6. *Efnb2* and *Shh* genetically interact to control progenitor numbers.

Transverse sections of E11.5 embryos of different genotypes (as indicated in the graph) were immunostained for Olig2 and Nkx2.2 and the number of Olig2+, Nkx2.2+ and Olig2+/Nkx2.2+ (double) progenitors was quantified for each genotype (n=5 embryos per genotype). Total refers to the sum of Olig2+ and Nkx2.2+ progenitors. Error bars indicate s.e.m.; **P<0.05*; ***P<0.01*; (unpaired two-sample *t*-tests).

Figure 7. Activation of EphA4 up-regulates *Nkx2.2* expression in primary spinal progenitors.

A. Primary spinal progenitors grown as neurospheres were immunostained with Tuj1 (neurons, green in a) and GFAP (astrocytes, red in a); Islet 1/2 (MN, red in b); Foxp1 (LMC MN, green in b); Olig2 (pMN and oligodendrocyte progenitors, green in c) and Nkx2.2 (p3 progenitors, red in c). Nuclei are stained with Draq5 (blue, a-c). B. Expression levels of

various genes (indicated) in primary spinal progenitors were analyzed by qRT-PCR. The graph is representative of three independent primary cultures C. Primary spinal progenitors were incubated for 2 h with either pre-clustered IgG-Fc, EfnB-Fc (EfnB2-Fc or EfnB3-Fc) or EphB2-Fc. Expression levels of different genes (indicated) was analyzed by qRT-PCR in all conditions. The graphs show fold change in expression levels comparing the control condition (IgG-Fc) and either EfnB-Fc (a) or EphB2-Fc (b) stimulations. Error bars indicate s.e.m.; n=5 experiments from 3 independent primary cultures; ***P<0.01; ***P<0.001*; (unpaired two-sample *t*-tests). Scale bars: 50 μm.

Figure 1, Laussu et al.

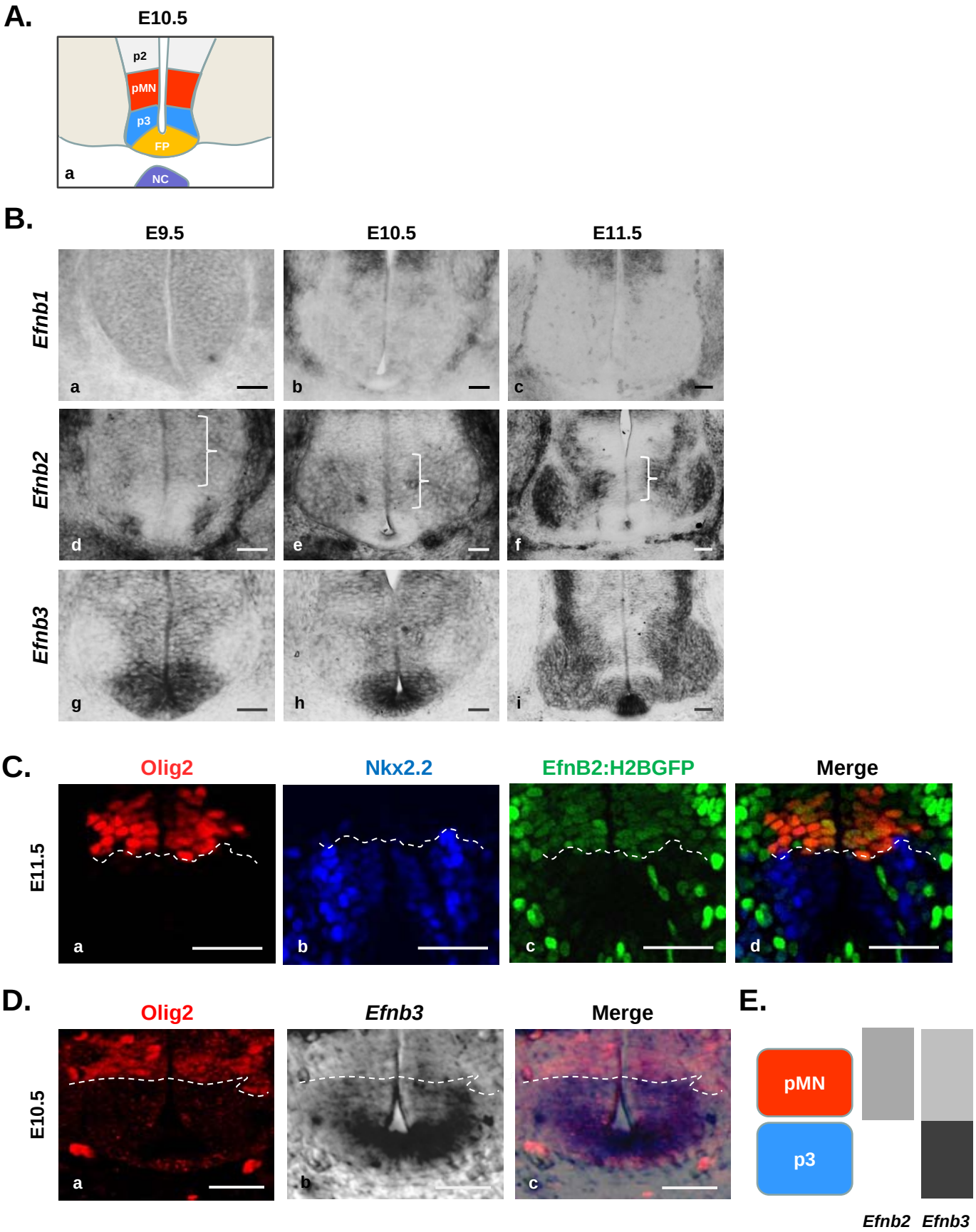

Figure 2, Laussu et al.

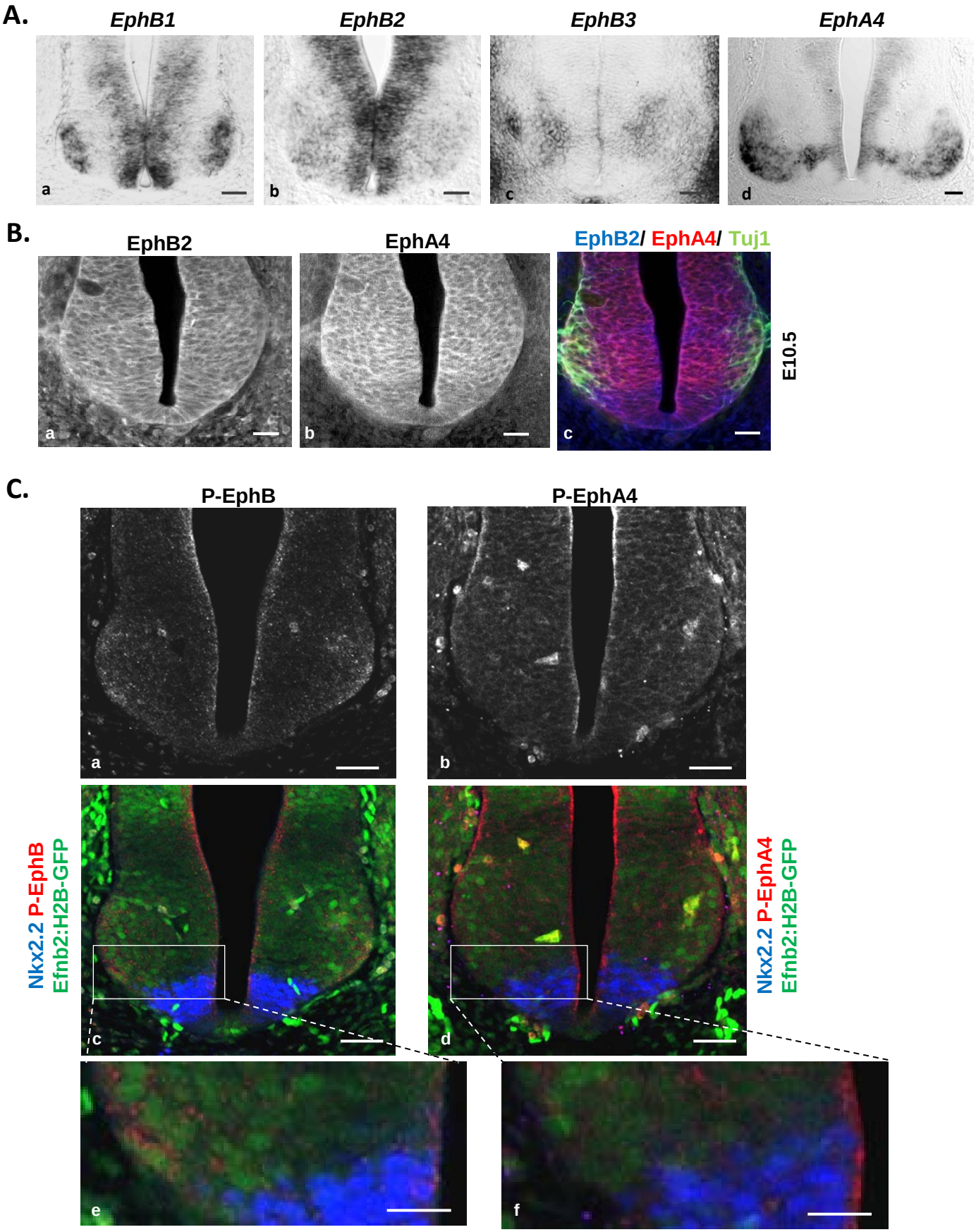

Figure 3, Laussu et al.

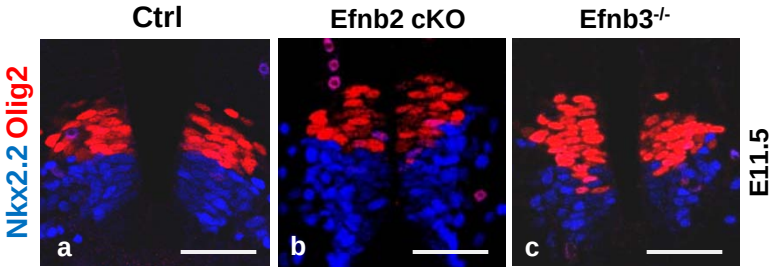

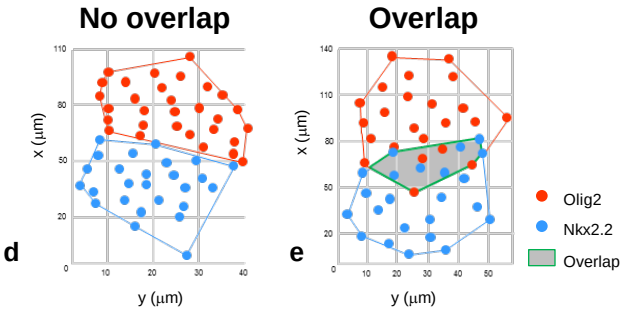

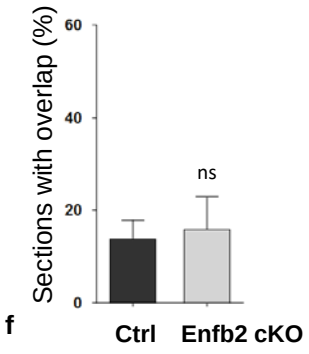

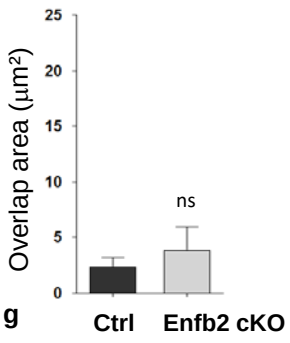

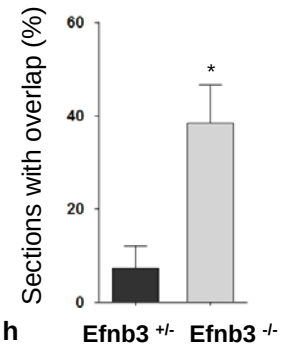

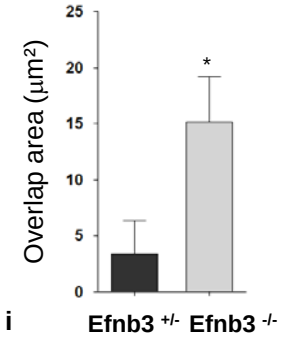

Figure 4, Laussu et al.

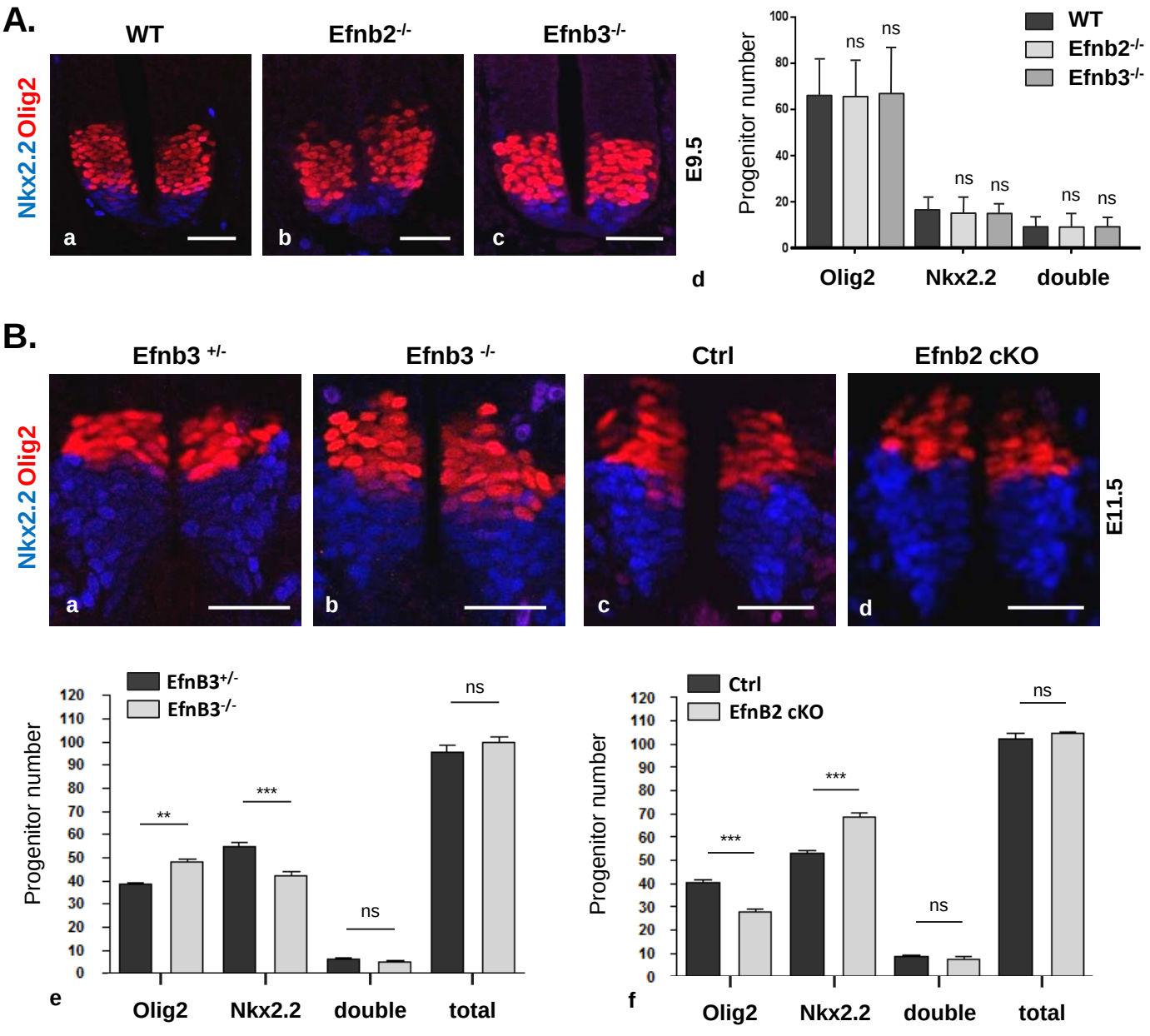

Figure 5, Laussu et al.

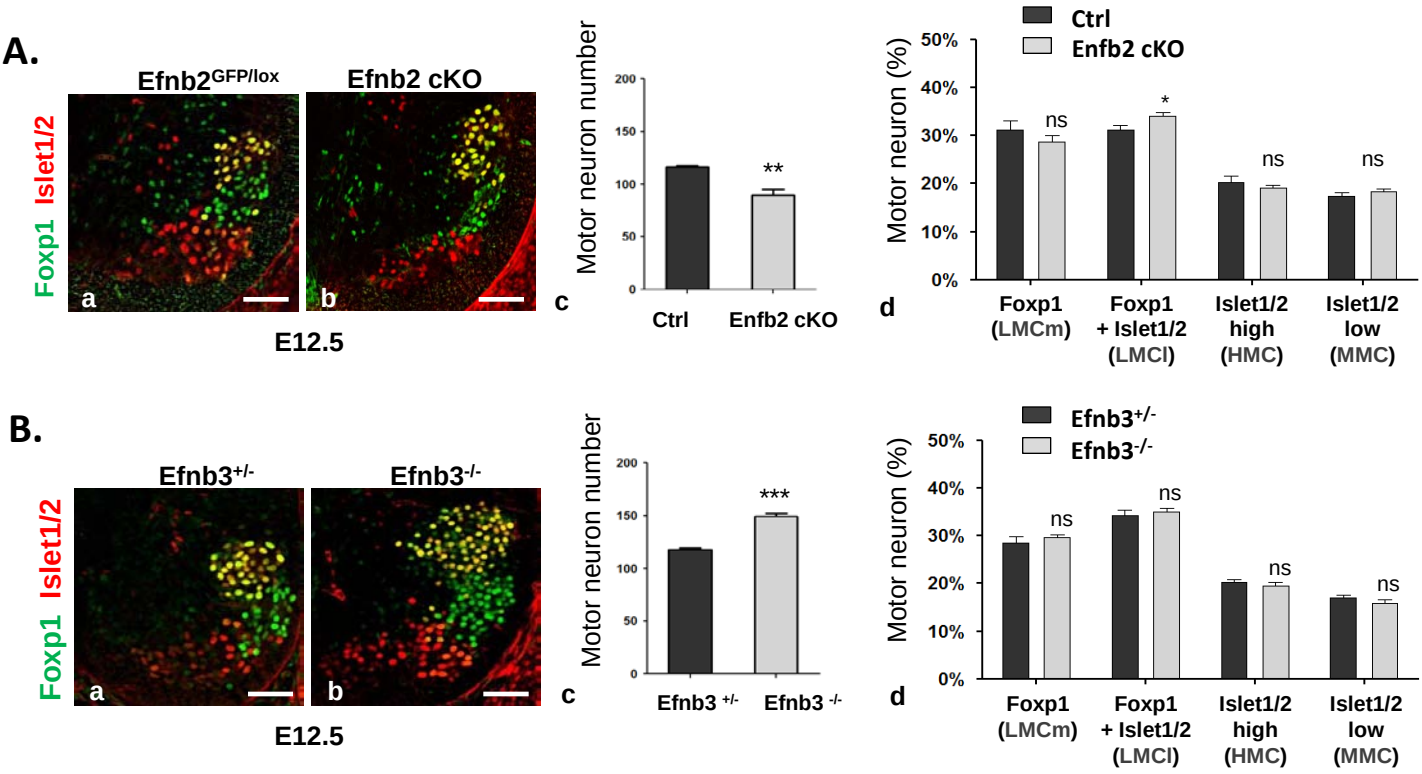

Figure 6, Laussu et al.

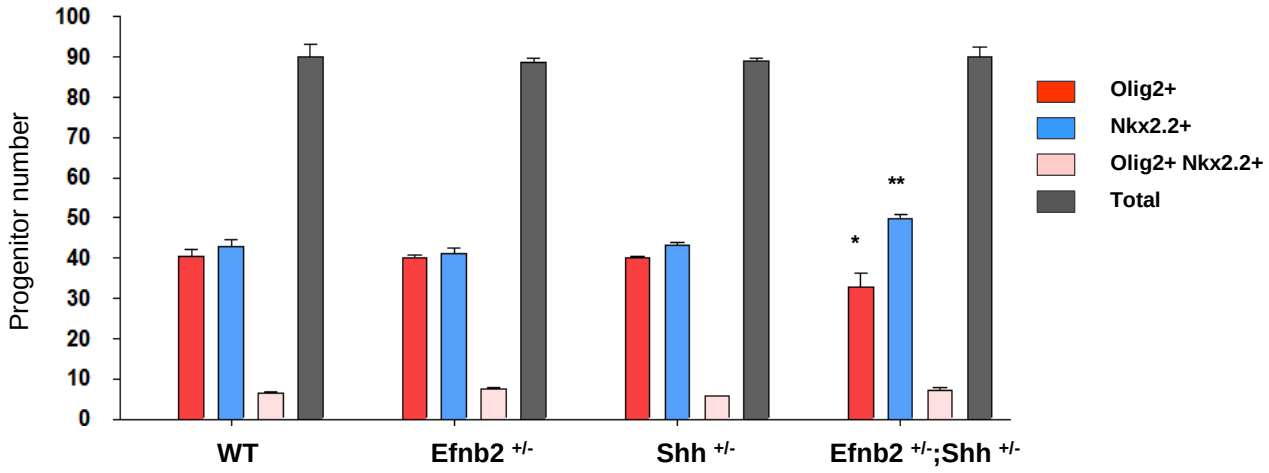

Figure 7, Laussu et al.

A.

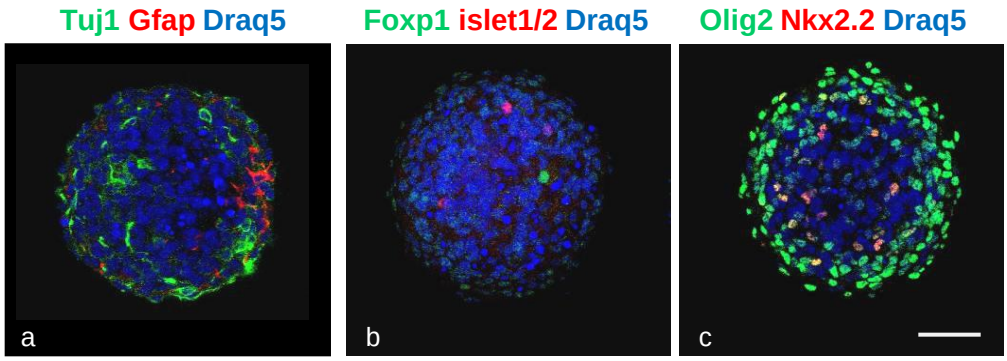

B.

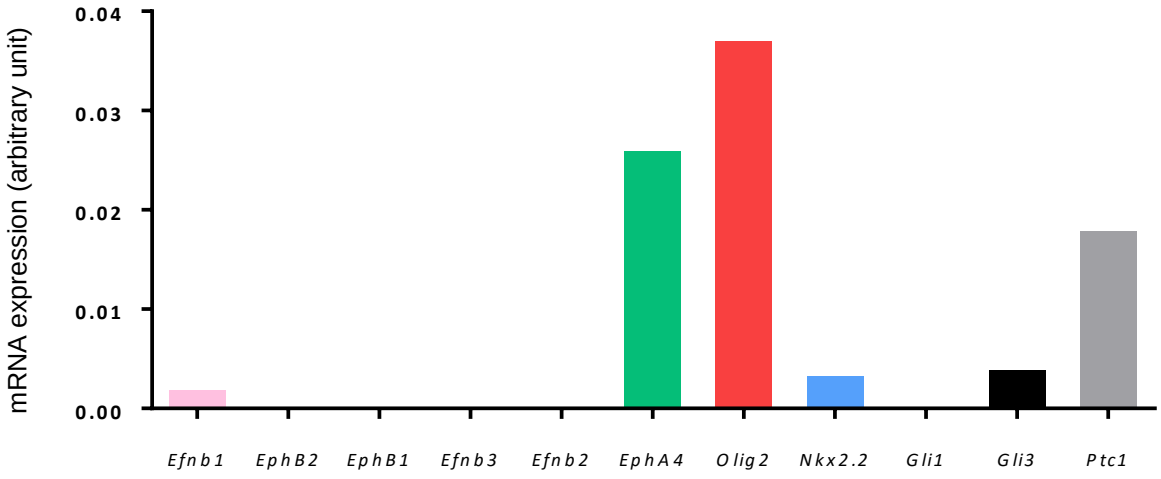

C.

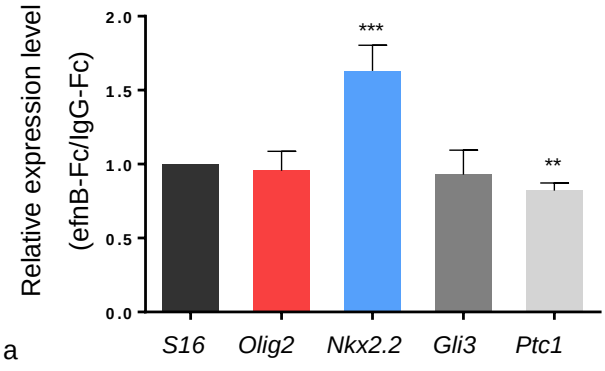

a

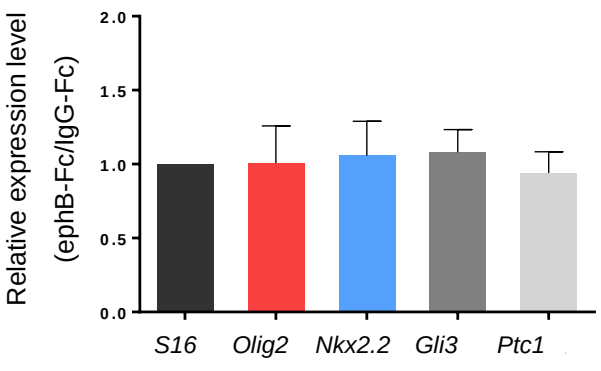

b